

Nonequilibrium chaos of disordered nonlinear waves

Ch. Skokos* and I. Gkolias

Physics Department, Aristotle University of Thessaloniki, GR-54124, Thessaloniki, Greece

S. Flach

*New Zealand Institute for Advanced Study, Centre for Theoretical
Chemistry and Physics, Massey University, Auckland, New Zealand*

(Dated: December 10, 2017)

Do nonlinear waves destroy Anderson localization? Computational and experimental studies yield subdiffusive nonequilibrium wave packet spreading. Chaotic dynamics and phase decoherence assumptions are used for explaining the data. We perform a quantitative analysis of the nonequilibrium chaos assumption, and compute the time dependence of main chaos indicators - Lyapunov exponents and deviation vector distributions. We find a slowing down of chaotic dynamics, which does not cross over into regular dynamics up to the largest observed time scales, still being fast enough to allow for a thermalization of the spreading wave packet. Strongly localized chaotic spots meander through the system as time evolves. Our findings confirm for the first time that nonequilibrium chaos and phase decoherence persist, fueling the prediction of a complete delocalization.

PACS numbers: 05.45-a, 05.60.Cd, 63.20.Pw

Introduction. In one and two dimensions, wave packets of noninteracting particles subject to a random potential on a lattice do not propagate due to exponential Anderson localization of the corresponding eigenstates [1, 2]. Anderson localization is a highly intriguing wave phenomenon, and has been recently probed in experiments on ultracold atomic gases in optical potentials [3, 4]. The wave localization effect is completely relying on keeping the phase coherence of participating waves. The presence of interaction between the particles may change this picture qualitatively. For many weakly interacting particles this is often taken into account by adding nonlinear terms to the linear wave equations of the noninteracting particles [5].

Numerical simulations of wave packets propagating in random lattice potentials showed the destruction of localization and a subdiffusive growth of the second moment of the wave packet in time as t^γ [6–16]. In particular, it was predicted that, for asymptotically large t , the coefficient γ should converge to $1/(1 + \sigma d)$ in the so-called ‘weak chaos’ regime, where d is the dimension of the lattice, and $\sigma + 1$ is the exponent of the nonlinear term in the wave equation (note that usual two-body interactions yield cubic nonlinear terms with $\sigma = 2$) [9, 10, 17]. A transient ‘strong chaos’ regime was also predicted [17] and observed [13, 14] where $\gamma = 2/(2 + \sigma d)$. Remarkably the onset of subdiffusive spreading was also experimentally detected for interacting ultracold atoms in optical potentials [18].

The main dynamical origin of the observed subdiffusion is believed to be deterministic chaos. Indeed, assume that a wave packet which is exciting a few lattice sites (or more) is not spreading. Then the dynamics of this trapped excitation can be described within a Hamiltonian system with a finite number of degrees of freedom,

which is nonlinear, and typically not integrable [19]. Excluding very weak nonlinearities and the Kolmogorov-Arnold-Moser (KAM) regime, the dynamics should be chaotic. Since deterministic chaos deteriorates correlations and leads to a decoherence of the wave phases, the main ingredient of Anderson localization is lost, and the wave packet can not be anymore localized [20]. Therefore one contradicts the initial assumption of persistence of localization. The wave packet can not keep its localization, but will spread. From this it also follows, that for weak enough nonlinearity the initially excited wave packet is in a KAM regime, where there is a finite probability to start on a chaotic trajectory, but with a finite complementary probability to end up on a regular trajectory which enjoys phase coherence and localization [19]. Indeed it was recently shown that the probability for chaos is practically equal to one above a nonlinearity threshold, and less than one below that threshold, tending towards zero in the limit of vanishing nonlinearity, thus restoring Anderson localization in this probabilistic sense [21]. The microscopic origin of chaos is expected to be hidden in the chaotic seeds of nonlinear resonances, which will fluctuate in time and space as the wave packet spreads [22].

To summarize, two main assumptions - the deterministic chaoticity of the wave packet dynamics, and the space-time fluctuation of the chaotic seeds - have to be confirmed to provide solid grounds for subdiffusion theories. A study of the interrelation between the appearance of chaos for nonlinear waves in the disordered Schrödinger equation was performed by Mulansky et al. [23]. Various relations between mode energies and capabilities to reach thermal equilibrium were studied for small systems, but not for the nonequilibrium wave packet spreading situation. In [24] it has been shown that chaoticity does not

necessarily imply thermalization for small-size disordered lattices. Michaely and Fishman [25] recently studied the temporal and frequency characteristics of effective nonlinear forces inside the wave packet, and concluded that these forces show sufficient randomness to qualify as effective noise terms - which is thought to be a result of deterministic chaos (but not a direct proof of its existence). Similarly Vermersch and Garreau [26] measured a spectral entropy, which however is only a very rough indicator for chaos. They also attempted to measure Lyapunov exponents, but only on short times. Moreover, all these attempts do not account for the *temporal dependence* of chaos strength. Indeed, the more the wave packet spreads, the weaker the chaos should become, since densities decrease. This is also reflected in the fact that the packets spread subdiffusively. Therefore we need a temporal resolution of the chaos indicators. That is what we will present in this work.

Model, equations and methods of analysis. The spreading of wave packets was numerically studied in a number of classes of wave equations. These equations share a surprising universality in that only the dimensionality of the lattice and the nonlinearity power σ influence the value of the exponent γ . Therefore we choose a chain of coupled anharmonic oscillators with random harmonic frequencies which belongs to the class of quartic Klein-Gordon (KG) lattices. This model is dynamically very similar to nonlinear Schrödinger equations with random potentials for small densities [9, 10, 13–15, 21, 27]. The Hamiltonian of the quartic KG chain of coupled anharmonic oscillators with coordinates u_l and momenta p_l is

$$\mathcal{H}_K = \sum_l \frac{p_l^2}{2} + \frac{\tilde{\epsilon}_l}{2} u_l^2 + \frac{1}{4} u_l^4 + \frac{1}{2W} (u_{l+1} - u_l)^2. \quad (1)$$

The equations of motion are $\ddot{u}_l = -\partial\mathcal{H}_K/\partial u_l$, and $\tilde{\epsilon}_l$ are chosen uniformly from the interval $[\frac{1}{2}, \frac{3}{2}]$. The value of \mathcal{H}_K serves as a control parameter of the system's nonlinearity. In the absence of the quartic term in (1) the ansatz $u_l(t) = A_l e^{i\omega t}$ yields the linear eigenvalue problem $\lambda A_l = \epsilon_l A_l - (A_{l+1} + A_{l-1})$ with $\epsilon_l = W(\tilde{\epsilon}_l - 1)$ and $\lambda = W(\omega^2 - 1) - 2$. This eigenvalue problem corresponds precisely to the well known Anderson localization in a one-dimensional chain with diagonal disorder [1, 2].

We analyze normalized energy distributions $\epsilon_l \geq 0$ using the second moment $m_2 = \sum_l (l - \bar{l})^2 \epsilon_l$, which quantifies the wave packet's degree of spreading and the participation number $P = 1/\sum_l \epsilon_l^2$, which measures the number of the strongest excited sites in ϵ_l . Here $\bar{l} = \sum_l l \epsilon_l$ and $\epsilon_l \equiv h_l/\mathcal{H}_K$ with $h_l = p_l^2/2 + \tilde{\epsilon}_l u_l^2/2 + u_l^4/4 + (u_{l+1} - u_l)^2/4W$. During the wave packet evolution we further estimate the maximum Lyapunov exponent (mLE) Λ_1 as the limit for $t \rightarrow \infty$ of the quantity $\Lambda(t) = t^{-1} \ln(\|\vec{v}(t)\|/\|\vec{v}(0)\|)$, often called *finite time mLE* [28–30]. $\vec{v}(0)$, $\vec{v}(t)$ are deviation vectors from a given trajectory, at times $t = 0$ and $t > 0$ respectively,

and $\|\cdot\|$ denotes the usual vector norm. $\Lambda(t)$ is a widely used chaos indicator. It tends to zero in the case of regular motion as $\Lambda^r(t) \sim t^{-1}$ [30, 31], while it tends to nonzero values for chaotic motion. Its inverse, T_L , is the characteristic timescale of the studied dynamical system, the so-called Lyapunov time. It quantifies the time needed for the system to become chaotic. The vector $\vec{v}(t)$ has as coordinates small deviations from the studied trajectory in positions and momenta ($v_i = \delta u_i$, $v_{i+N} = \delta p_i$, $1 \leq i \leq N$, N being the total number of lattice sites). Its time evolution is governed by the so-called variational equations. In our study we also compute normalized deviation vector distributions (DVDs) $w_l = (v_l^2 + v_{l+N}^2)/\sum_l (v_l^2 + v_{l+N}^2)$.

We use the symplectic integrator SABA₂ with corrector [10, 32] for the integration of the equations of motion, and its extension according to the so-called tangent map method [33–35] for the integration of the variational equations. We considered lattices with $N = 1000$ to $N = 2000$ sites in our computations, in order to exclude finite-size effects in the evolution of the wave packets, and an integration time step $\tau = 0.2$, which kept the relative energy error always less than 10^{-4} .

Results. In Fig.1(a) we first study the single trajectory of a single site excitation with total energy $E = 0.4$ and $W = 4$ (case I) which is known to evolve in the asymptotic regime of ‘weak chaos’ [9, 10, 13]. We show the time dependence of the second moment (red curve) and observe the expected subdiffusive growth $m_2 \sim t^{1/3}$. The simulation of a single site excitation in the absence of nonlinear terms (orange curve) corresponds to regular motion and Anderson localization is observed. In Fig.1(b) we plot the time dependence of $\Lambda(t)$ for the two cases of Fig.1(a). At variance to the t^{-1} decay for the regular nonchaotic trajectory (orange curve), the observed decay for the ‘weak chaos’ orbit is much weaker and well fitted with $\Lambda \sim t^{-1/4}$ (red curve).

We substantiate the findings of Fig.1(b) by averaging $\log_{10} \Lambda$ over 50 realizations of disorder and extending to two more ‘weak chaos’ parameter cases with initial energy density $\epsilon = 0.01$ distributed evenly among a block of 21 central sites for $W = 4$ (case II) and 37 central sites for $W = 3$ (case III). All cases show convergence towards $\Lambda \sim t^{-1/4}$ (Fig.1(c)). We further differentiate the curves in Fig.1(c) following the approach used in [13, 14], estimate their slope $\alpha_L = \frac{d(\log_{10} \Lambda(t))}{d \log_{10} t}$, and show the result in Fig.1(d) which underpin the above findings. Therefore

$$\Lambda(t) \sim t^{-1/4} \gg \frac{1}{t}. \quad (2)$$

So far we have clear numerical proof that the dynamics inside the spreading wave packet remains chaotic up to the largest simulation times, without any tendency towards regular dynamics. As expected, the chaoticity diminishes in time due to the decrease of the energy density

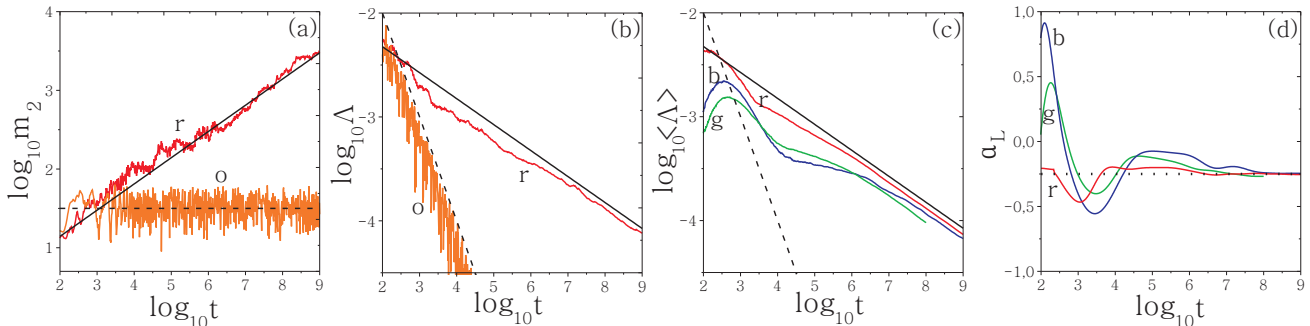


FIG. 1: (Color online) (a) Time evolution of the second moment m_2 for one disorder realization of an initially single site excitation with $E = 0.4$, $W = 4$ (Case I), in log – log scale (red (r) curve). The orange (o) curve corresponds to the solution of the linear equations of motion, where the term u_i^4 in Eq.(1) is absent. Straight lines guide the eye for slopes $1/3$ (solid line) and 0 (dashed line). (b) Time evolution of the finite time maximum Lyapunov exponent Λ (multiplied by 10 for the orange (o) curve) for the trajectories of panel (a) in log – log scale. The straight lines guide the eye for slope -1 (dashed line), and $-1/4$ (solid line). (c) Time evolution of the averaged Λ over 50 disorder realizations for the ‘weak chaos’ cases I, II and III [(r) red; (b) blue; (g) green] (see text for more details). Straight lines guide the eye for slopes -1 and $-1/4$ as in panel (b). (d) Numerically computed slopes α_L of the three curves of panel (c). The horizontal dotted line denotes the value $-1/4$.

inside the spreading wave packet. Therefore, complete chaotization and randomization of phases inside the wave packet will take more time, the more the packet spreads. To substantiate the assumptions needed for subdiffusive spreading theories, we will compare the Lyapunov time T_L (estimated by $1/\Lambda$) with the time scales which characterize the subdiffusive spreading. A first time scale of this kind, T_D , can be obtained from the growth of the second moment $m_2 \sim t^{1/3}$. It follows that the inverse of this timescale, i.e. the effective diffusion coefficient D , is a function of the densities, and decays in time as [27]

$$\frac{1}{T_D} = D \sim t^{-2/3}, \quad \Lambda \gg D, \quad \frac{T_D}{T_L} \sim t^{5/12}. \quad (3)$$

A second time scale can be obtained by estimating a spreading time T_s given by the increase of P by one (site), i.e. $T_s \sim 1/\dot{P}$ (with $P \sim t^{1/6}$ [9, 10, 14]). Therefore

$$\frac{1}{T_s} \sim t^{-5/6}, \quad \Lambda \gg \frac{1}{T_s}, \quad \frac{T_s}{T_L} \sim t^{7/12}. \quad (4)$$

As it follows from Eqs.(2,3,4), the dynamics remains chaotic, and the chaoticity time scale is always shorter than the spreading time scales, and their ratio diverges as a power law. We thus confirm for the first time the assumption about persistent and fast enough chaoticity needed for subdiffusive spreading theories.

A second very important assumption for subdiffusive spreading theories is based on the fact that chaoticity is induced by nonlinear resonances inside the wave packet, which are the seeds of deterministic chaos and *have to meander* through the packet in the course of evolution [10, 22]. Indeed, assume that their spatial position is fixed. Then such seeds will act as spatially pinned ran-

dom force sources on their surrounding. The noise intensity of these centers will decay in time. At any given time the exterior of the wave packet is then assumed to be approximated by the linear wave equation part which enjoys Anderson localization. However, even for constant intensity it was shown [36] that the noise will not propagate into the system due to the dense discrete spectrum of the linear wave equation. Therefore the wave packet can only spread if the nonlinear resonance locations meander in space and time.

We visualize the motion of these chaotic seeds by following the spatial evolution of the deviation vector used for the computation of the mLE. This vector tends to align with the most unstable direction in the system’s phase space. Thus, monitoring how its components on the lattice sites evolve we can identify the most chaotic spots. Large DVD values tell us at which sites the sensitivity on initial conditions (which is a basic ingredient of chaos) is larger.

In Fig.2(a) we plot the energy density distribution for an individual trajectory of case I at three different times $t \approx 10^6, 10^7, 10^8$ and in Fig.2(b) the corresponding DVD. We obtain that the energy densities spread more evenly over the lattice the more the wave packet grows. At the same time the DVD stays localized, but the peak positions clearly meander in time, covering distances of the order of the wave packet width. The full time evolution of the energy density and the DVD is shown in Figs.2(c,d) together with the track of the distribution’s mean position (central white curve). While the energy density distribution shows a modest time dependence of the position of its mean, the DVD mean position is observed to perform fluctuations whose amplitude increases with

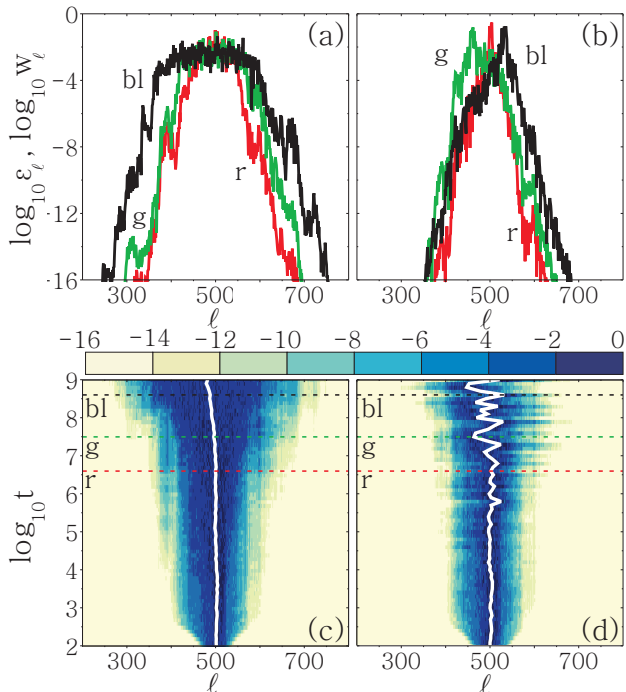


FIG. 2: (Color online) The dynamics of an individual trajectory of case I. Normalized (a) energy (ϵ_l) and (b) deviation vector (w_l) distributions at $t = 4 \times 10^6$, $t = 3 \times 10^7$, $t = 4 \times 10^8$ [(r) red; (g) green; (bl) black]. Time evolution of (c) the energy distribution and (d) the DVD for the realization of panel (a) in \log_{10} scale. The position of the distribution's mean position is traced by a thick white curve. The times at which the distributions of panels (a) and (b) are taken are denoted by straight horizontal lines in (c) and (d).

time.

Summary and discussion. We computed nonequilibrium chaos indicators of the spreading of wave packets in disordered lattices. For the first time we find that chaos not only exists, but also persists. Using a set of observables we are able to show that the slowing down of chaos does not cross over into regular dynamics, and is at all times fast enough to allow for a thermalization of the wave packet. Moreover the monitoring of the spatio-temporal dynamics of hot chaotic spots yields an increase in their spatial fluctuations - in accord with previous unproven assumptions.

The mLE decreases when the wave packet spreads, since the energy density decreases as well. Nevertheless, the mLE follows a completely different power law as compared to the case of regular motion. This signals the lack of sticking to regular structures in phase space, as conjectured recently [37, 38].

We also studied the spatial evolution of the deviation vector associated with the mLE. The corresponding distributions remain localized with a very pointy profile. This observation supports theoretical assumptions that

in the ‘weak chaos’ regime only few nonlinear resonances appear at a time. The mean position of these distributions performs random oscillations, whose amplitude increases as the wave packet spreads. These oscillations result in a homogeneity of chaos inside the packet, i.e. in thermalization.

All these findings clearly show that nonlinear wave packets spread in random potentials due to deterministic chaos and dephasing. Moreover, wave packets first thermalize, and only later perform subdiffusive spreading. That is a basic prerequisite for the existing theoretical description of energy spreading in disordered nonlinear lattices, and the applicability of nonlinear diffusion equations [27, 39–41].

Acknowledgments. Ch.S. and S.F. thank the Max Planck Institute for the Physics of Complex Systems in Dresden, Germany for its hospitality during their visits, when part of this work was carried out. Ch.S. was supported by the Research Committee of the Aristotle University of Thessaloniki (Prog. No 89317), and by the European Union (European Social Fund - ESF) and Greek national funds through the Operational Program “Education and Lifelong Learning” of the National Strategic Reference Framework (NSRF) - Research Funding Program: “THALES. Investing in knowledge society through the European Social Fund”. The HellasGrid infrastructure was used for the numerical simulations.

* Electronic address: hskokos@auth.gr

- [1] P. W. Anderson, Phys. Rev. **109**, 1492 (1958).
- [2] B. Kramer and A. MacKinnon, Rep. Prog. Phys. **56**, 1469 (1993).
- [3] J. Billy et al., Nature **453**, 891 (2008).
- [4] G. Roati et al., Nature **453**, 895 (2008).
- [5] L. P. Pitaevsky and S. Stringari, Bose-Einstein Condensation, Oxford University Press, Oxford (2003).
- [6] G. Kopidakis, S. Komineas, S. Flach and S. Aubry, Phys. Rev. Lett. **100**, 084103 (2008).
- [7] A. S. Pikovsky and D. L. Shepelyansky, Phys. Rev. Lett. **100**, 094101 (2008).
- [8] I. García-Mata and D. L. Shepelyansky, Phys. Rev. E **79**, 026205 (2009).
- [9] S. Flach, D. O. Krimer, and Ch. Skokos, Phys. Rev. Lett. **102**, 024101 (2009).
- [10] Ch. Skokos, D. O. Krimer, S. Komineas and S. Flach, Phys. Rev. E **79**, 056211 (2009).
- [11] H. Veksler, Y. Krivolapov and S. Fishman, Phys. Rev. E **80**, 037201 (2009).
- [12] Ch. Skokos and S. Flach, Phys. Rev. E **82**, 016208 (2010).
- [13] T. V. Lapyteva, J. D. Bodyfelt, D. O. Krimer, Ch. Skokos, and S. Flach, EPL **91**, 30001 (2010).
- [14] J. D. Bodyfelt, T. V. Lapyteva, Ch. Skokos, D. O. Krimer, and S. Flach, Phys. Rev. E **84**, 016205 (2011).
- [15] T. V. Lapyteva, J. D. Bodyfelt and S. Flach, EPL **98**, 6002 (2012).
- [16] G. Gligoric, K. Rayanov and S. Flach, EPL **101**, 10011 (2013).

- [17] S. Flach, Chem. Phys. **375**, 548 (2010).
- [18] E. Lucioni et al., Phys. Rev. Lett. **106**, 230403 (2011).
- [19] M. C. Gutzwiller, Chaos in Classical and Quantum Mechanics, Springer, Berlin (1990).
- [20] K. Rayanov, G. Radons and S. Flach, Phys. Rev. E, in print; arXiv:1301.4307 (2013).
- [21] M. V. Ivanchenko, T. V. Lapyteva and S. Flach, Phys. Rev. Lett. **107**, 240602 (2011).
- [22] D. O. Krimer and S. Flach, Phys. Rev. E **82**, 046221 (2010).
- [23] M. Mulansky, K. Ahnert, A. Pikovsky and D. L. Shepelyansky, Phys. Rev. E **80**, 056212 (2009).
- [24] O. Tieleman, Ch. Skokos and A. Lazarides, arXiv:1306.2810 (2013).
- [25] E. Michaely and S. Fishman, Phys. Rev. E **85**, 046218 (2012).
- [26] B. Vermersch and J. C. Garreau, New J. Phys. **15** 045030 (2013). (2013).
- [27] T. V. Lapyteva, J. D. Bodyfelt and S. Flach, Physica D **256-257**, 1 (2013).
- [28] G. Benettin, L. Galgani, A. Giorgilli and J.-M. Strelcyn, Meccanica **15**, 9 (1980).
- [29] G. Benettin, L. Galgani, A. Giorgilli and J.-M. Strelcyn, Meccanica **15**, 21 (1980).
- [30] Ch. Skokos, Lect. Notes Phys. **790**, 63 (2010).
- [31] G. Benettin, L. Galgani and J.-M. Strelcyn, Phys. Rev. A **14**, 2338 (1976).
- [32] J. Laskar and P. Robutel, Celest. Mech. Dyn. Astron. **80**, 39 (2001).
- [33] Ch. Skokos and E. Gerlach, Phys. Rev. E, **82**, 036704 (2010).
- [34] E. Gerlach and Ch. Skokos, Discr. Cont. Dyn. Syst. - Ser. A, Supp., 457 (2011).
- [35] E. Gerlach, S. Eggl and Ch. Skokos, Int. J. Bifurcation Chaos, **22**, 1250216 (2012).
- [36] S. Aubry and R. Schilling, Physica D **238**, 2045 (2009).
- [37] M. Johansson, G. Kopidakis, and S. Aubry, EPL **91**, 50001 (2010).
- [38] S. Aubry, Int. J. Bifurcation Chaos, **21**, 2125 (2011).
- [39] M. Mulansky and A. Pikovsky, EPL **90**, 10015 (2009).
- [40] M. Mulansky and A. Pikovsky, New J. Phys. **15**, 053015 (2013).
- [41] E. Lucioni et al, Phys. Rev. E **87**, 042922 (2013).